A Gα-Stimulated RapGEF Is a Receptor-Proximal Regulator of Dictyostelium Chemotaxis

Liu, Youtao; Lacal, Jesus; Veltman, Douwe M; Fusetti, Fabrizia; van Haastert, Peter J M; Firtel, Richard A; Kortholt, Arjan

Published in:
Developmental Cell

DOI:
10.1016/j.devcel.2016.05.001

Article

Developmental Cell

A Gα-Stimulated RapGEF Is a Receptor-Proximal Regulator of *Dictyostelium* Chemotaxis

Highlights

- The Rap1GEF GlfB is a receptor-proximal regulator of chemotaxis in *Dictyostelium*
- GflB localizes to the leading edge and is stimulated directly by Gα-GTP binding
- GflB directly links Gα activation to monomeric G-protein signaling
- GflB provides a mechanism to discriminate between distinct chemoattractants

Authors

Youtao Liu, Jesus Lacal, Douwe M. Veltman, Fabrizia Fusetti, Peter J.M. van Haastert, Richard A. Firtel, Arjan Kortholt

Correspondence

a.kortholt@rug.nl

In Brief

G-protein-coupled receptors (GPCRs) mediate chemotaxis via activation of linked G proteins. Although many signaling pathways downstream of Gβγ are known, less is known about Gα. Liu, Lacal et al. identify a *Dictyostelium* Rap1GEF that binds Gα and thereby links the cAMP GPCR to Rap1, regulating cytoskeletal dynamics and chemotaxis.

Liu et al., 2016, Developmental Cell *37*, 458–472
June 6, 2016
http://dx.doi.org/10.1016/j.devcel.2016.05.001

CellPress

CellPress

Developmental Cell
Article

A Gα-Stimulated RapGEF Is a Receptor-Proximal Regulator of *Dictyostelium* Chemotaxis

Youtao Liu,[1,5] Jesus Lacal,[2,5] Douwe M. Veltman,[3] Fabrizia Fusetti,[4] Peter J.M. van Haastert,[1] Richard A. Firtel,[2,6] and Arjan Kortholt[1,6,*]

[1]Department of Cell Biochemistry, University of Groningen, Nijenborgh 7, 9747 AG Groningen, the Netherlands
[2]Section of Cell and Developmental Biology, Division of Biological Sciences, University of California, San Diego, La Jolla, CA 92093, USA
[3]MRC Laboratory of Molecular Biology, Cambridge CB2 0QH, UK
[4]Department of Biochemistry, Netherlands Proteomics Centre, Groningen Biological Sciences and Biotechnology Institute, University of Groningen, 9747 AG Groningen, the Netherlands
[5]Co-first author
[6]Co-senior author
*Correspondence: a.kortholt@rug.nl
http://dx.doi.org/10.1016/j.devcel.2016.05.001

SUMMARY

Chemotaxis, or directional movement toward extracellular chemical gradients, is an important property of cells that is mediated through G-protein-coupled receptors (GPCRs). Although many chemotaxis pathways downstream of Gβγ have been identified, few Gα effectors are known. Gα effectors are of particular importance because they allow the cell to distinguish signals downstream of distinct chemoattractant GPCRs. Here we identify GflB, a Gα2 binding partner that directly couples the *Dictyostelium* cyclic AMP GPCR to Rap1. GflB localizes to the leading edge and functions as a Gα-stimulated, Rap1-specific guanine nucleotide exchange factor required to balance Ras and Rap signaling. The kinetics of GflB translocation are fine-tuned by GSK-3 phosphorylation. Cells lacking GflB display impaired Rap1/Ras signaling and actin and myosin dynamics, resulting in defective chemotaxis. Our observations demonstrate that GflB is an essential upstream regulator of chemoattractant-mediated cell polarity and cytoskeletal reorganization functioning to directly link Gα activation to monomeric G-protein signaling.

INTRODUCTION

Chemotaxis, or directional movement toward an extracellular chemical gradient, is fundamentally important for processes as diverse as innate immunity, food foraging, and organogenesis (Artemenko et al., 2014). During the last decade, important progress has been made by elucidating a complex network of interconnecting signaling pathways controlling amoeboid cell chemotaxis, mainly through the use of *Dictyostelium* and mammalian neutrophils as experimental systems (Artemenko et al., 2014; Nichols et al., 2015). Activation of G-protein-coupled receptor (GPCR)-linked heterotrimeric G protein by guanosine diphosphate/triphosphate (GDP/GTP) exchange in the Gα subunit results in the dissociation into Gα-GTP and a Gβγ subunit, and the activation of the Rho/Rac and Ras families of monomeric G proteins (Faix and Weber, 2013; Jin, 2013; Kortholt et al., 2013; Sasaki and Firtel, 2009). Positive and negative feedback and feedforward loops lead to the intracellular amplification of the extracellular chemoattractant gradient that includes the preferential localization of activated Rac, Ras, and Rap1 at the leading edge, which results in major changes in the cytoskeleton with actin polymerization at the leading edge and actin-myosin filament assembly at the rear and sides of the cell (Artemenko et al., 2014).

Many chemotaxis pathways that are directly regulated by Gβγ have been identified, including: human phosphatidylinositol 3-kinase γ (PI3Kγ; phosphatidylinositol (3,4,5)-trisphosphate [PIP_3] production) (Stephens et al., 2008); *Dictyostelium* ElmoE, which, with Dock proteins, activates RacB (Yan et al., 2012); Dock2, which activates Rac1 and Rac2 (Kunisaki et al., 2006); and phospholipase Cβ, which hydrolyzes phosphatidylinositol (4,5)-bisphosphate (PIP_2) to DAG and inositol trisphosphate (Tang et al., 2011). However, we are only beginning to understand whether Gα-GDP/GTP exchange mediates downstream signaling mainly through the release of Gβγ and/or whether distinct signaling pathways are regulated through different Gα subunits. Recently, some mammalian Gα effectors important for chemotaxis were identified, including Dock180, a Rac activator highly homologous to Dock2 (Li et al., 2013), the scaffolding protein mInsc (Kamakura et al., 2013), and Homer3, a Gαi2-binding protein that spatially helps organizes actin assembly (Wu et al., 2015).

Using a combination of proteomic approaches in *Dictyostelium* (Kataria et al., 2013; Kölsch et al., 2013), we identify GflB as a Gα2-GTP interacting protein and GSK-3 substrate that is required for efficient directional sensing and cell movement during chemotaxis. Our findings indicate that GflB is a Gα-stimulated, Rap1-specific guanine nucleotide exchange factor (GEF) that plays a central role for the balance between Ras and Rap signaling at the leading edge of chemotaxing cells.

RESULTS AND DISCUSSION

GflB Plays a Role in Gα2-Mediated Chemotaxis

We identified *Dictyostelium* GflB (GEF-like protein B), with six unique and specific peptides that were not present in control

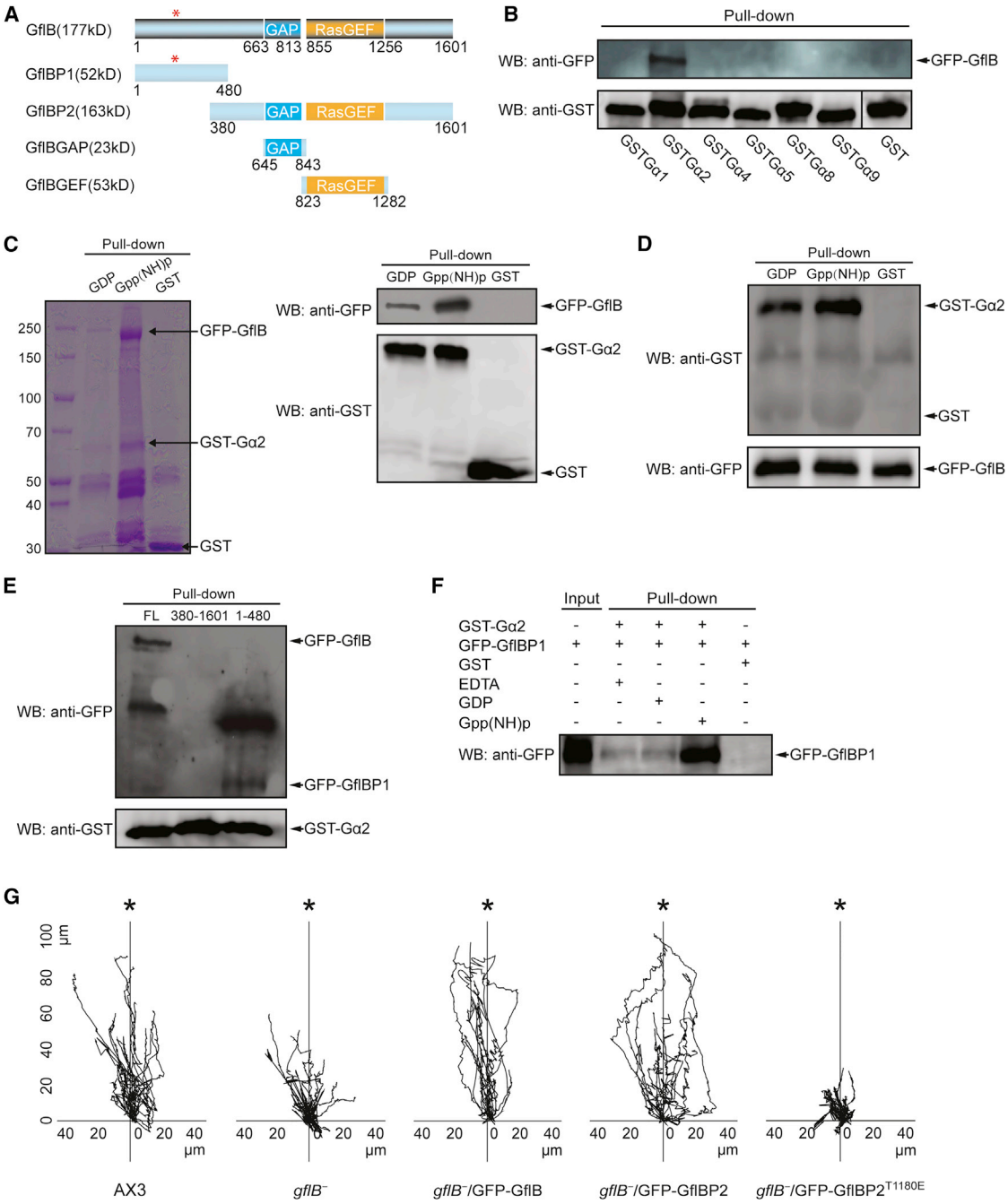

Figure 1. GflB Is a Gα2-Specific Effector Important for Chemotaxis

(A) Domain topology and schematic representation of GflB and its truncated versions used in this study. The GSK-3 phosphorylation site (197 and 201 amino acids) is indicated with an asterisk.

(B) Physical association of full-length GflB and Gα(s). Glutathione Sepharose beads coated with GST and GST-Gα1, 2, 4, 5, 8, and 9 were incubated with GFP-GflB cell lysate. GFP and GST tags were detected by western blotting as described in Experimental Procedures. A representative western blot of three independent experiments is shown.

(C) GflB binds to Gα2 in vivo. Lysates of GFP-GflB/GST-Gα2, or GFP-GflB/GST co-expressed *gflB*$^{-}$ cells were subjected to GSH beads in the presence of either 100 μM Gpp(NH)p or 100 μM GDP. Bound proteins were resolved by stained SDS-PAGE and visualized by Coomassie blue (left panel) or western blot (right panel) with anti-GST and anti-GFP antibodies. Representative images of three independent experiments are shown.

(D) GflB binds preferentially to GTP-bound Gα2 using GFP-GflB as bait. GFP-GflB was bound to GFP antibody pre-coupled protein A magnetic beads, followed by the incubation of GST-Gα2 cell lysate in the presence of either 100 μM Gpp(NH)p or 100 μM GDP. Proteins were detected by western blot with anti-GST and anti-GFP antibodies. A representative western blot of three independent experiments is shown.

(legend continued on next page)

samples (pulled down with glutathione S-transferase [GST] protein), in a proteomic analysis of potential Gα2 binding partners (Kataria et al., 2013) and independently as a potential GSK-3 substrate through a comparison of the phosphoproteome of wild-type and *gskA*$^-$ (GSK-3) null cells (Kölsch et al., 2013). Interestingly, GflB contains both a putative Rho GTPase-activating protein (RhoGAP) domain (663–813 amino acids) and a putative Ras guanine nucleotide exchange factor (RasGEF) domain (855–1,256 amino acids) (Figure 1A).

To confirm GflB binding to and specificity for Gα2, we expressed GFP-tagged GflB full-length protein in *Dictyostelium* and performed pull-down experiments with recombinant, purified GST-fused Gα proteins. Figure 1B illustrates that GFP-GflB binds to GST-Gα2 but not to the other tested *Dictyostelium* Gα proteins, including Gα4, which controls chemotaxis downstream of the *Dictyostelium* folate chemoattractant GPCR (Hadwiger et al., 1994), nor to free GST, suggesting that GflB interacts specifically with Gα2 (Figure 1B). To address binding in vivo and determine the nucleotide specificity, we co-expressed GFP-GflB and GST-Gα2 in *Dictyostelium* cells and performed pull-down experiments in the presence of GDP or GppNHp (Figure 1C). Importantly, western blots show that GFP-GflB preferentially binds to active GST-Gα2 (GppNHp bound) compared with inactive (GDP-bound) GST-Gα2. Pull-downs with GFP-GflB as bait consistently revealed much stronger binding to GppNHp-loaded GST-Gα2 compared with GDP-loaded Gα2 (Figure 1D). To investigate which GflB domain interacts with Gα2, we generated truncated constructs that either contain the N-terminal fragment (GFP-GflBP1) or the GflB GAP and GEF domains (GflBP2) (Figure 1A). Immunoprecipitation analyses showed that active GST-Gα2 (GppNHp bound) preferentially binds to GFP-GflBP1, while we observed no detectable binding of GFP-GflBP2 to active or inactive GST-Gα2 (Figures 1E and 1F).

Dictyostelium Gα2 binds to the high-affinity cyclic AMP (cAMP) receptor (cAR1) and is responsible for almost all cAMP-mediated responses (Kumagai et al., 1989). To characterize the function of GflB in vivo, we generated a *gflB*-null (*gflB*$^-$) strain by homologous recombination. Consistent with the specific interaction of GflB with Gα2, GflB does not play a major role during vegetative growth: *gflB*$^-$ cells do not show any defect in cell growth, macropinocytosis, Rac activation, or folate chemotaxis (Figures S1A–S1C). Interestingly, cells expressing GflBP2 show multiple patches of active Rac and severely reduced growth, and become multi-nucleated (Figures S1A–S1C, see also below). Next we quantified the ability of wild-type and *gflB*$^-$ cells to chemotax to cAMP using a micropipette assay (Meili et al., 1999). *gflB*$^-$ cells show only slightly reduced cAR1 expression compared with wild-type cells, indicating that they are sufficiently developed to respond to cAMP (Figure S1D). Whereas wild-type cells chemotax efficiently up a gradient of cAMP, *gflB*$^-$ cells exhibit considerable chemotaxis defects, including poorer directionality, more directional changes, and slower speed compared with wild-type cells (Table 1 and Figure 1G). Overexpression of GFP-tagged GflB complements the *gflB*$^-$ cells' chemotaxis defects (Table 1; Figure 1G; Movies S1, S2, and S3). As expected from the chemotaxis defects, *gflB*$^-$ cells exhibit severe developmental defects (Figure S1E). While wild-type cells form streams and aggregate between 5 and 8 hr after plating on non-nutrient agar plates, *gflB*$^-$ cells form delayed, smaller aggregates that mostly do not form fruiting bodies (Figure S1E). In contrast, overexpressing GFP-tagged GflB in *gflB*$^-$ results in slightly faster development compared with wild-type cells.

GflB Is a Gα2-Dependent Rap1-Specific GEF

One of the first downstream responses of heterotrimeric G-protein signaling is the activation of small G proteins (Kae et al., 2004; Kortholt and van Haastert, 2008; Sasaki and Firtel, 2006) that rapidly switch between an inactive (GDP-bound) and active (GTP-bound) state with only the GTP-bound form being able to bind to downstream effectors (Bourne et al., 1991). For small G proteins, the switch between the GTP-bound active and GDP-bound inactive states is controlled by GEFs and GAPs, which stimulate the low intrinsic GTPase activity of the G proteins (Trahey and McCormick, 1987). GflB contains both a putative RhoGAP domain and a putative RasGEF domain (Figure 1A). However, the RhoGAP domain sequence contains notable changes in the catalytic domain (Figure S2A) compared with known GAPs, including a substitution of the invariant Arg required for GAP activity (Zhang et al., 1999). We show that although the GflB GAP domain is able to bind several Rac proteins, this binding is nucleotide independent (Figures S2B–S2D). These findings strongly suggest that GflB, like human OCRL and *Dictyostelium* Dd5P4 (Loovers et al., 2007), contains an inactive RhoGAP domain.

To address the function of the GflB RasGEF domain, we generated a construct containing an inactivating mutation in the RasGEF domain (GFP-GflBP2^{T1180E}) (Vanoni et al., 1999). *gflB*$^-$ cells overexpressing GFP-GflBP2^{T1180E} have similar reduced directionality compared with *gflB*$^-$ cells (Table 1 and Figure 1G), demonstrating an essential role for an active RasGEF domain in GflB signaling.

The *Dictyostelium* Ras GTPase subfamily comprises 11 Ras, three Rap, and one Rheb-related protein (Weeks et al., 2005).

(E) Gα2 binds to the N terminus of GflB. Lysates of *gflB*$^-$ cells expressing GFP-GflB (full length), GFP-GflBP2 (380–1,601), and GFP-GflBP1 (1–480) were incubated with GST-Gα2-bound GSH beads in the presence of Gpp(NH)p. Pull-down eluates were immunoblotted with anti-GST and anti-GFP antibodies. A representative western blot of three independent experiments is shown.

(F) GFP-GflBP1 binds preferentially to GTP-bound Gα2. GFP-GflBP1 cell lysate was incubated with GST-Gα2 bound glutathione Sepharose beads were pre-incubated with either 100 μM Gpp(NH)p, 100 μM GDP, or 10 mM EDTA. Pull-down eluates were immunoblotted with anti-GFP antibody. A representative western blot of three independent experiments is shown.

(G) "Spider" plots of wild-type (AX3) and *gflB*$^-$, *gflB*$^-$/GFP-GflB, *gflB*$^-$/GFP-GflBP2, and *gflB*$^-$/GFP-GflBP2^{T1180E} cells migrating toward the tip of a needle (indicated by the asterisks) containing 10 μM of the chemoattractant cAMP. Tracks of individual cells (n = 19) are shown as lines for all strains. These tracks were generated using individual cells from five independent experiments. A total elapse time of 15 min (150 frames; each frame was pictured every 6 s) was used to plot the x and y positions of the centroid of the cells, which were computed over the 150 frames using DIAS.

See also Figures S1 and S2.

Table 1. DIAS Analysis of Representative Developed Cells Performing Chemotaxis to 1 μM cAMP

Cell Strains	Directionality	Speed (μm/min)	Direction Change	Roundness (%)
AX3	0.60 ± 0.13	7.65 ± 1.44	42.29 ± 9.29	39.38 ± 3.77
gflB$^-$	0.20 ± 0.06**	4.02 ± 0.49*	65.40 ± 4.56**	47.50 ± 8.20
gflB$^-$/GFP-GflB	0.74 ± 0.05	8.42 ± 1.15	29.65 ± 5.82*	47.15 ± 4.08*
gflB$^-$/GFP-GflBP2	0.67 ± 0.11	11.26 ± 2.26**	37.58 ± 10.49	48.14 ± 7.62*
gflB$^-$/GFP-GflBP2^{T1180E}	0.39 ± 0.18**	7.35 ± 2.38	55.20 ± 9.68**	48.48 ± 11.09*

Data represent analysis performed with 12 different cells from five independent experiments ± SD, for each strain. Speed refers to the speed of the cell's centroid movement along the total path; directionality indicates migration straightness; direction change refers to the number and frequency of turns; and roundness indicates cell polarity. *$p < 0.05$, **$p < 0.01$, Student's t test. The chemotaxis defects shown result in severe developmental defects. See also Figure S1.

Thus far, five Ras proteins (RasB, RasC, RasD, RasG, and RasS) and one Rap (Rap1) have been characterized to some extent, and they all appear to have important roles in cell physiology (Kortholt and van Haastert, 2008). Although one cannot presently predict the specificity of putative RasGEFs based on sequence, the in vitro specificity of GEFs can be directly examined using a nucleotide exchange assay (Figure 2A). Purified GST-tagged Rap1 and RasG were loaded with [^{3}H]GDP and an excess of cold GDP was then added, and the nucleotide exchange was measured as the decay in radioactivity associated with the G protein. Addition of recombinant GST-GflB-GEF (644–1,282 amino acids) to [^{3}H]GDP-labeled Rap1 results in a rapid decrease in bound [^{3}H]GDP, indicating an acceleration of the intrinsic low nucleotide exchange activity of Rap1 (Figure 2A). However, GflB-GEF is unable to stimulate the nucleotide exchange of functional [^{3}H]GDP-labeled RasG (Figure 2A) (Kortholt et al., 2006), suggesting that GflB may have specificity for Rap1 in vitro. Consistent with this conclusion, immunoprecipitation experiments reveal that GflB-GEF binds to nucleotide free Rap1, whereas we detected no binding to nucleotide-free RasB, RasC, RasD, RasG, or RasS (Figure S2E).

Although GflBP2 efficiently binds Rap1, we detected little binding of full-length GflB to Rap1 (Figure 2B). As the N terminus of GflB interacts with active Gα2, we performed pull-down experiments with full-length GflB in the presence or absence of active Gα2. GST-tagged GflB was expressed in *Dictyostelium* cells and used as bait in a lysate of *Dictyostelium* cells expressing GFP-Rap1. Figure 2B shows that GflB binds efficiently to GFP-Rap1 only in the presence of active Gα2. These data suggest that binding of active Gα2 releases an auto-inhibition of the N terminus, thereby allowing GflB to bind Rap1, and that GflB is thus a Gα2-GTP stimulated, Rap1-specific GEF.

gflB$^-$ Cells Exhibit Decreased Rap1 and Increased Ras Activation

Figure S3A shows that N-terminal GFP-fused Rap1 and RasG are localized mainly at the cell membrane of both wild-type and *gflB*$^-$ cells. To monitor spatial activation of the protein, rather than its localization, we quantified cAMP-stimulated Rap1 activation in cell lysates using pull-down assays with GST-RalGDS and imaged them in vivo using the RalGDS-GFP reporter (Matsubara et al., 1999). As previously reported (Jeon et al., 2007a), we found that wild-type cells exhibit a low basal level of Rap1-GTP that rises rapidly in response to global chemoattractant stimulation with a peak at ~5 s and then returns quickly to basal levels (Figures 2C and 2D). Currently it is not known how cAMP-mediated Rap activation is regulated, since the two identified Rap1-specific GEFs, GbpD and GEFQ, are mainly important for Rap-mediated adhesion in vegetative cells and cytoskeletal rearrangement at the poles of dividing cells (Kortholt et al., 2006; Plak et al., 2014). In contrast, and consistent with GflB being a Gα2-mediated Rap1 GEF, *gflB*$^-$ cells exhibit severely impaired Rap1 activation in response to cAMP (Figures 2C and 2D).

We next quantitated Ras activation in wild-type and *gflB*$^-$ cells using pull-down assays with GST-Raf1-RBD or GST-Byr2 as bait, and Ras activation was imaged in vivo with a Raf1-RBD-GFP marker as described previously (Kortholt et al., 2011). GST-Raf1-RBD preferentially binds RasG and RasB, while GST-Byr2 binds strongest to RasC (Kae et al., 2004; Zhang et al., 2008). Wild-type cells exhibit a low basal level of Ras-GTP, which rises rapidly in response to global chemoattractant stimulation with a peak at ~5 s and then returns quickly to basal levels (Figures 2E and 2F). The highly sensitive pull-down assays showed that *gflB*$^-$ cells have high basal levels of active Ras in vitro and, both in vitro and in vivo, have an elevated and extended cAMP-mediated Ras response compared with that in wild-type cells.

In a cAMP gradient, wild-type cells are polarized, and both RalGDS-GFP and Raf1-RBD-GFP rapidly accumulate at the side of the cell facing the gradient (Figures 2D and 2F, right panels). We calculated the ratio of fluorescence at the cell cortex in the up-gradient half of the cell to that in the down-gradient half of the cell (Figure S3B; Kortholt et al., 2011). Wild-type cells show 7.28 ± 2.79-fold ($n = 8$) and 8.73 ± 0.75-fold ($n = 8$) more Rap1 and Ras activation, respectively, at the front half compared with the back half of the cell. *gflB*$^-$ cells have a less polarized Ras (2.98 ± 0.54, $n = 8$, $p < 0.0001$) and Rap1 (4.00 ± 1.31, $n = 8$, $p < 0.05$) response compared with wild-type cells (Figure S3B). In steep gradients of cAMP, the initial wide bell-shaped curve of membrane-bound Raf1-RBD-GFP becomes very narrow (7.53 ± 0.55 μm), with very steep flanks. In contrast, this confinement is absent in *gflB*$^-$ cells, resulting in a much broader Ras crescent (12.46 ± 1.44 μm, $n = 8$, $p < 0.0001$) compared with that in wild-type cells, indicating an inability to effectively polarize in a chemoattractant gradient. Confinement of Ras signaling depends on cytoskeleton rearrangement (Kortholt et al., 2013), a process that is coordinated by Rap1 (Jeon et al., 2007a).

Our findings suggest that GflB is involved in the regulation of the balance between Ras and Rap signaling at the leading edge of chemotaxing cells.

GflB Is Required for Proper Regulation of Chemotaxis Pathways

Both Ras and Rap1 are upstream regulators of the PI3K and TORC2 pathways that play critical roles in directional sensing, cytoskeletal reorganization, and cell movement (Arthur et al., 2004; Bolourani et al., 2006; Charest et al., 2010; Funamoto et al., 2002; Lee et al., 2005; Mun and Jeon, 2012; Plak et al., 2013; Sasaki and Firtel, 2006; Sasaki et al., 2004; Takeda et al., 2007).

We analyzed the kinetics of PI3K activation, which is an effector of RasG and Rap1 (Funamoto et al., 2002; Kortholt et al., 2010), using the PIP_3 reporter PH_{CRAC}-GFP (Insall et al., 1994). In wild-type cells, PH_{CRAC}-GFP is predominantly cytosolic in unstimulated cells and rapidly localizes to the plasma membrane in response to uniform cAMP stimulation and to the leading edge in chemotaxing cells (Figure 3A). *gflB*$^-$ cells exhibit an extended plasma membrane localization of PH_{CRAC}-GFP in response to cAMP stimulation compared with wild-type cells. Furthermore, these cells exhibit a high, uniformly distributed PH_{CRAC}-GFP over the entire cell periphery prior to stimulation and also during chemotaxis as well as in vegetative cells, suggesting a high, uniform basal PI3K activity, consistent with elevated an elevated basal RasG activity (Figure 3A). Consistent with these observations, we find that cAMP-stimulated PI3K cortical localization is extended in *gflB*$^-$ cells compared with that in wild-type cells, and is found along the entire cortex already prior to stimulation and also during chemotaxis rather than localized at the leading edge (Figure S4A). These results agree with the lack of apparent polarization in developed *gflB*$^-$ cells, as described above.

Akt/PKB and the related enzyme PKBR1 play key roles in regulating leading edge function during chemotaxis (Meili et al., 1999, 2000; Kamimura et al., 2008). Akt/PKB and PKBR1 are activated at the plasma membrane by two phosphorylations, as are mammalian Akt/PKBs (Sarbassov et al., 2005): their activation loops (ALs) are phosphorylated by the two PDK1 isoforms (Kamimura et al., 2008; Liao et al., 2010), whereas TORC2, an effector of RasC, phosphorylates the conserved hydrophobic motif (HM) (Cai and Devreotes, 2011; Charest et al., 2010; Kamimura et al., 2008; Lee et al., 2005). Chemoattractant-mediated plasma membrane localization of Akt/PKB is mediated through the binding of its PH domain to the PI3K product PIP_3 (Meili et al., 1999; Funamoto et al., 2002) while PKBR1 is constitutively localized on the plasma membrane through an N-terminal myristoyl group (Meili et al., 2000; Lee et al., 2005; Kamimura et al., 2008). In cAMP-responsive wild-type cells, the AL and HM phosphorylation of Akt/PKB and PKBR1 peak at ~10 s after chemoattractant stimulation, consistent with the peak of kinase activity (Figures 3B and 3C) (Meili et al., 2000; Lee et al., 2005; Kamimura et al., 2008). In *gflB*$^-$ cells, the AL phosphorylation is elevated and extended for Akt/PKB and PKBR1, and the phosphorylation of the HM is also elevated and extended (Figures 3B and 3C). Consistent with these findings, several substrates of Akt/PKB have extended phosphorylation in response to cAMP stimulation in *gflB*$^-$ cells (Figure S4B). These observations are consistent with elevated basal RasG and RasC activities and elevated and extended cAMP-stimulated activity.

GflB Regulates cAMP-Induced Myosin II Assembly and Actin Polymerization

Spatially localized activation of Rap1 and Ras induces F-actin polymerization at the leading edge of chemotaxing cells through the Rac, PI3K, and TORC2 pathways described above (Artemenko et al., 2014; Jin, 2013). At the same time, active Rap1 inhibits myosin assembly at the leading edge through activation of its effector Phg2, while low levels of active Rap1 at the side and back of the cell allow myosin formation (Jeon et al., 2007a, 2007b). Thus, the balance in the temporal and spatial regulation of Ras and Rap1 activation is essential to control both actin and myosin rearrangements during chemotaxis (Artemenko et al., 2014). Consistent with the increased RasG response, we find that F-actin polymerization is elevated in *gflB*$^-$ cells compared with that in wild-type cells, whereas myosin II (MyoII) assembly is dramatically reduced compared with that in wild-type cells (Figures 4A–4C). Overexpression of GFP-GflB or GflBP2 complements these *gflB*$^-$ cell phenotypes (Figures 4A–4C). Furthermore, in wild-type cells the F-actin reporter Lifeact-GFP is found at a low level along the cell cortex in unstimulated cells, predominantly at small protrusions, and is transiently localized along the whole cell cortex in response to uniform cAMP stimulation (Figure 4D). In chemotaxing wild-type cells, the reporter is enriched at the leading edge while *gflB*$^-$ cells exhibit a higher basal and more uniformly distributed level of Lifeact-GFP at the cortex before and after cAMP stimulation, consistent with the elevated F-actin in *gflB*$^-$ cells. In addition, the basal and cortically localized levels of MyoII are dramatically decreased in *gflB*$^-$ cells compared with those in wild-type cells (Figure 4E). As expected, GFP-MyoII is enriched at the rear and sides of the migrating wild-type cells but is not detectable at the cortex in *gflB*$^-$ cells (Figure 4F). Together, our findings demonstrate that GflB has an important role in regulating Ras- and Rap1-mediated F-actin and myosin dynamics at the leading edge of chemotaxing cells.

The N Terminus Functions to Regulate Both GflB-GEF Activity and Its Localization

To further understand the activation mechanism of GflB, we analyzed the function and localization of full-length, truncated, and mutated versions of GflB. In developed, randomly moving cells, GflB is mainly in the cytoplasm except for a few patches of increased fluorescence observed at the cell boundary at the sites of protrusions (Figure 5A). During chemotaxis, GflB localizes at the leading edge of cells (Figure 5A), whereas in response to uniform (global) cAMP stimulation, GFP-GflB rapidly and transiently translocates to the cortex (Figure 5A). The kinetics of the GflB translocation are more accurately monitored by computational analysis of fluorescence intensity depletion in the cytoplasm (Figure 5B). The translocation of GFP-GflB starts immediately upon cAMP stimulation, peaks at ~8 s, and returns to basal levels by ~18 s. Because GflB localization seems to be thicker than that defined by plasma membrane as observed with Raf1-RBD-GFP or PH_{CRAC}-GFP (Figure 5A), and GflB regulates actin-myosin dynamics, we investigated a role for the cell cortex in regulation. In cells incubated with the actin-polymerization inhibitor latrunculin A (LatA), GflB does not translocate to the cell

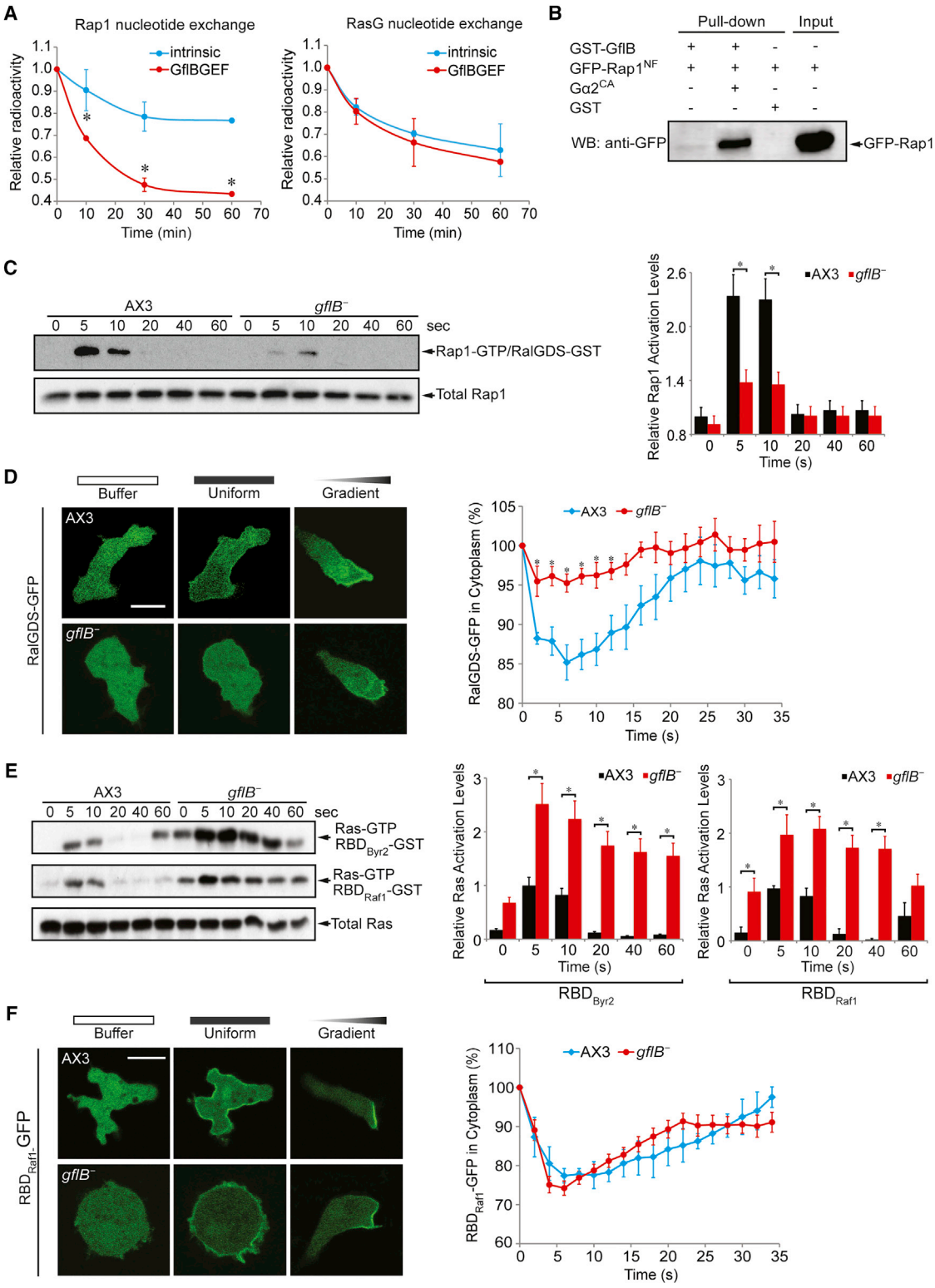

Figure 2. GflB Is a Gα2-Dependent Rap1-Specific GEF

(A) Rap1 and RasG [^{3}H]GDP release with (red line) and without (blue line) GflB-GEF in the presence of an excess of GDP. Data are mean and SD of at least three independent experiments; significantly different from control without GflB-GEF at *$p < 0.05$ (Student's t test).

(legend continued on next page)

boundary on uniform cAMP stimulation (Figure 5B), suggesting that localization depends on a functional cytoskeleton. Previous reports have shown that cytoskeleton-associated GAP proteins are important for the regulation of Rap1 activity (Jeon et al., 2007a). Consistent with these results, we find that addition of LatA to starved cells results in a strong uniform Rap1 response that does not increase further upon addition of cAMP (Figure S4D). In contrast, LatA does not induce a uniform Rap1 response in *gflB*$^{-}$ cells, suggesting that GflB is required for cytoskeletal regulation of Rap1 activation. Furthermore, addition of LatA to *gflB*$^{-}$ cells completely restores the prolonged cAMP-mediated Ras response in *gflB*-null cells, while it does not affect the amplitude or kinetics of the Ras response in wild-type cells (Figure S4E). These data show that the observed Ras phenotype of *gflB*$^{-}$ cells depends on a functional cytoskeleton and that GflB, consistent with our biochemical data (Figure S2E), indirectly regulates Ras activity.

Interestingly, the constitutively active GflBP2 fragment (see above) is already localized at the cortex before stimulation, and we detect no further increase of fluorescence after global stimulation with cAMP (Figure 5B). Similarly, in unstimulated cells the N terminus of GflB (GflBP1) also localizes to the cell boundary; however, the localization of GflBP1 does not change in the presence of LatA, suggesting that GflBP1 is bound to the membrane rather than the cytoskeleton (Figure 5C). The binding of GflBP1 to the membrane most likely involves interaction with lipids (Figure S5A).

Together, these results suggest that translocation of GflB is initiated by binding of activated Gα2 to the GflB N terminus, resulting in exposure of a lipid binding site in GflB, resulting in a more stable binding to the plasma membrane at the sites of activated Gα2. This interaction then allows the binding of a now active GflBP2 to the cell cortex via interaction with Rap1 and/or other sites on the cortex. At the same time, RapGAPs accumulate at the cortex at the back of the cell (Jeon et al., 2007b). This spatial separation of GEFs and GAPs subsequently leads to Rap activation in a large area at the front of the cell.

GSK-3 Phosphorylation Modulates GflB Localization

A comparative bioinformatics screening of a total cell phosphoproteomic analysis (tandem mass spectrometry array) of developed wild-type and GSK-3-null (*gskA*$^{-}$) cells in response to cAMP stimulation shows that GflB is not phosphorylated at a potential GSK-3 site in *gskA*$^{-}$ cells (Figure S5B). GflB is simultaneously phosphorylated at Ser^{197} (putative GSK-3 site) and Thr^{201} (putative priming site) before (0 s, basal), at 10 s (the time of maximum activation of many leading edge pathways), and at 60 s (adaptation) after cAMP stimulation in wild-type, but no phosphorylation at these sites is observed in *gskA*$^{-}$ cells (Figure S5B). Indeed, we identified the same phosphorylation sites in a previous proteomics screening in wild-type cells (Charest et al., 2010). In addition, peptides containing phospho-Ser^{197} (but not phospho-Thr^{201}) are only identified at 60 s after cAMP stimulation, suggesting that GSK-3 might regulate GflB adaptation rather than its activation in response to the chemoattractant. Our study detects other phosphorylations on GflB in *gskA*$^{-}$ cells, suggesting that the lack of phosphorylation at the potential GSK-3 site is probably due to the absence of GSK-3 rather than GflB not being detected. We verified that GflB is a direct target of GSK-3 by examining the ability of immunoprecipitated T7-GflB expressed in *gskA*$^{-}$ cells to be phosphorylated in an in vitro kinase assay by recombinant human GSK-3β (Figure 5D). Wild-type GflB and GflB carrying Ala substitutions at Ser^{197} and Thr^{201} (GflB$^{S197A/T201A}$) show similar low phosphorylation during the first 4 min, suggesting that GSK-3β can phosphorylate additional sites in vitro. However, at later time points GflB$^{S197A/T201A}$ is less phosphorylated than the wild-type protein, suggesting that Ser^{197} and Thr^{201} are the major sites of GSK-3β phosphorylation in vitro. We observed smaller differences in the phosphorylation of GflB and GflB$^{S197A/T201A}$ for incubation times longer than 10 min (Figure S5C). The in vitro kinase assay observations, together with the phosphoproteomics findings, identified a GSK-3 phosphorylation site in GflB, suggesting that GflB is a direct in vivo target for GSK-3, which is known to regulate MyoII function (Kölsch et al., 2013).

We examined the function of GflB phosphorylation by GSK-3 by expressing GFP-GflB in *gskA*$^{-}$ cells. In response to uniform cAMP concentration, the cortical translocation of GFP-GflB peaks more rapidly, and the level of accumulation is more elevated and extended than that of GFP-GflB in wild-type cells (Figure 5E, left panel). To determine whether phosphorylation of the identified GSK-3 site in GflB mediates this response, we expressed the non-phosphorylatable (GFP-GflB$^{S197A/T201A}$)

(B) Interaction between GflB and Rap1. GSH beads coated with GST-GflB were incubated with GFP-Rap1 EDTA-added cell lysate in the presence or absence of constitutively active Gα2. Immunoprecipitation was performed using an anti-GFP antibody. A representative western blot of three independent experiments is shown.

(C) The activation level of endogenous Rap1 in response to cAMP was assayed using GST-RalGDS pull-down assays. AX3 and *gflB*$^{-}$ cells were stimulated with 1 μM cAMP for the indicated times and analyzed by immunoblot assay using an antibody against Rap1. The quantification of the blots is shown in the right panel. Error bars represent average data for at least four independent experiments. For quantification, the starting point of wild-type cells was set as 1.0 and the data for the different time points in wild-type and *gflB*$^{-}$ cells were plotted relative to Rap1-GTP levels at this starting point. *$p < 0.05$ (Student's t test).

(D) Live images of RalGDS-GFP expressing AX3 and *gflB*$^{-}$ cells in buffer, 4–6 s after uniform stimulation with 1 μM cAMP and gradient stimulation with 10 μM cAMP. The relative cytoplasm fluorescence intensity of RalGDS-GFP is shown in the right panel, representing mean (n = 12) ± SEM of three independent experiments. *$p < 0.05$ (Student's t test). Scale bar represents 5 μm.

(E) The endogenous Ras activation was measured by GST-Byr2-RBD and GST-Raf1-RBD pull-down assays. Cells were stimulated with 1 μM cAMP for the indicated duration, and the amount of Ras protein bound to GST-RBD was determined by western blotting with an anti-pan-Ras antibody. The right panel shows the quantification of blots of at least three independent experiments indicating the relative activation of Ras in response to cAMP. All Ras activation time points are relative to time point 5 s (peak of activation) in wild-type cells. *$p < 0.05$ (Student's t test).

(F) In vivo live images using the Raf1-RBD-GFP reporter. Representative images of Raf1-RBD-GFP expressing cells in buffer, uniform stimulation with 1 μM cAMP, and gradient stimulation with 10 μM cAMP are shown in the left panel. Time course of Raf1-RBD-GFP translocation from the cytoplasm to the membrane are shown in the right panel. Data represent mean (n = 10) ± SEM of three independent experiments. Scale bar represents 5 μm.

See also Figures S2 and S3.

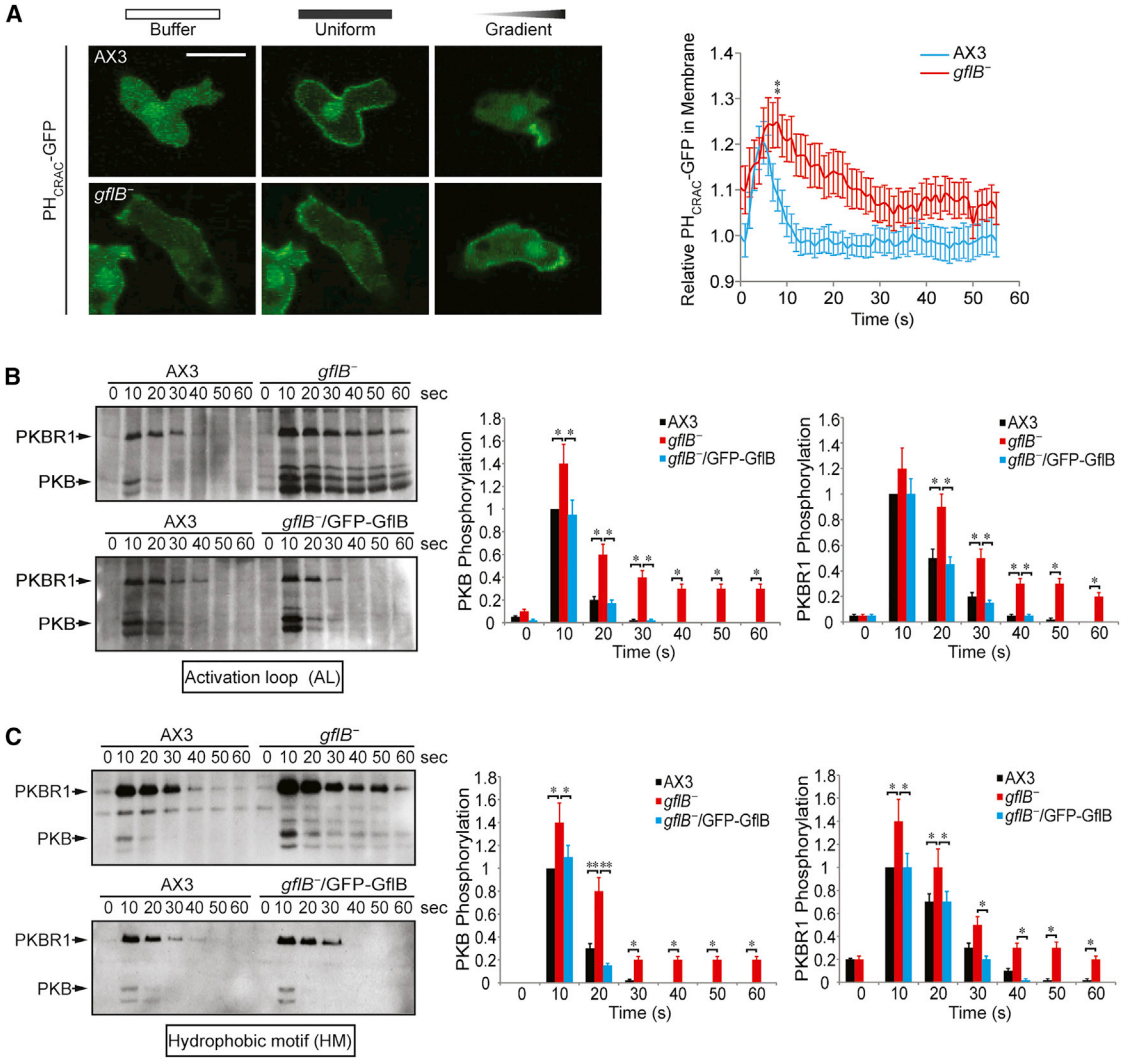

Figure 3. GflB Is Required for the Proper Regulation of the Chemotaxis Pathways

(A) Representative live images of translocation kinetics of a PIP3 reporter PH_{CRAC}-GFP in AX3 and *gflB*$^-$ cells, upon uniform (1 μM) and gradient (100 μM) cAMP stimulation. Scale bar represents 5 μm. The right panel shows quantification of the relative membrane fluorescence intensity of uniformly cAMP-stimulated PH_{CRAC}-GFP. Data represent mean (n = 15) ± SD of relative fluorescence intensity of membrane-localized PH_{CRAC}-GFP compared with unstimulated AX3 cells (t = 0) as a function of time after cAMP stimulation. **p < 0.01, Student's t test.

(B and C) Phosphorylation of the activation loop (AL) (B) and hydrophobic motif (HM) (C) of PKB and PKBR1 in AX3, *gflB*$^-$, and *gflB*$^-$ cells expressing GFP-GflB in response to 1 μM cAMP. The right panels show the quantification of AL (B) and HM (C) phosphorylation of PKB and PKBR1 normalized to the peak value of AX3 (t = 10 s), representing mean ± SD of three independent experiments. *p < 0.05, **p < 0.01, Student's t test.

See also Figure S4.

and the phosphomimetic form of GflB (GFP-GflB$^{S197D/T201D}$) in wild-type and *gflB*$^-$ cells. The cortical translocation of GFP-GflB$^{S197D/T201D}$ in *gflB*$^-$ cells is similar to that of wild-type GFP-GflB expressed in *gflB*$^-$ cells (Figure 5E, right panel). In contrast, we found that GFP-GflB$^{S197A/T201A}$ peaks more rapidly and the peak is slightly elevated and more extended than in wild-type GFP-GflB, similar to, but not as extreme as, our observations when GFP-GflB is expressed in *gskA*$^-$ cells (Figure 5E, right panel). We made similar observations for GFP-GflB$^{S197A/T201A}$ expressed in wild-type cells (Figure 5E). Together, these findings suggest that phosphorylation of the N terminus of GflB by GSK-3 results in less, delayed, and shorter GflB recruitment to the cortex. Thus, GSK3 phosphorylation is not essential for activation but helps modulate the extent and timing of the translocation.

Model for the Function of GflB

We demonstrate that GflB binds to and is activated by Gα2-GTP and directly links the cAMP receptor to Rap1 activation at the leading edge and, thus, one of the most receptor-proximal regulators of chemotaxis in this system. GflB is required for proper cell polarization, integration of Rap1 and Ras pathways, and the spatiotemporal regulation of the F-actin/myosin cytoskeleton (Figure 6A). GflB is a Rap1 GEF that is stimulated by direct binding to Gα. Interestingly, GflB appears to be specific to the

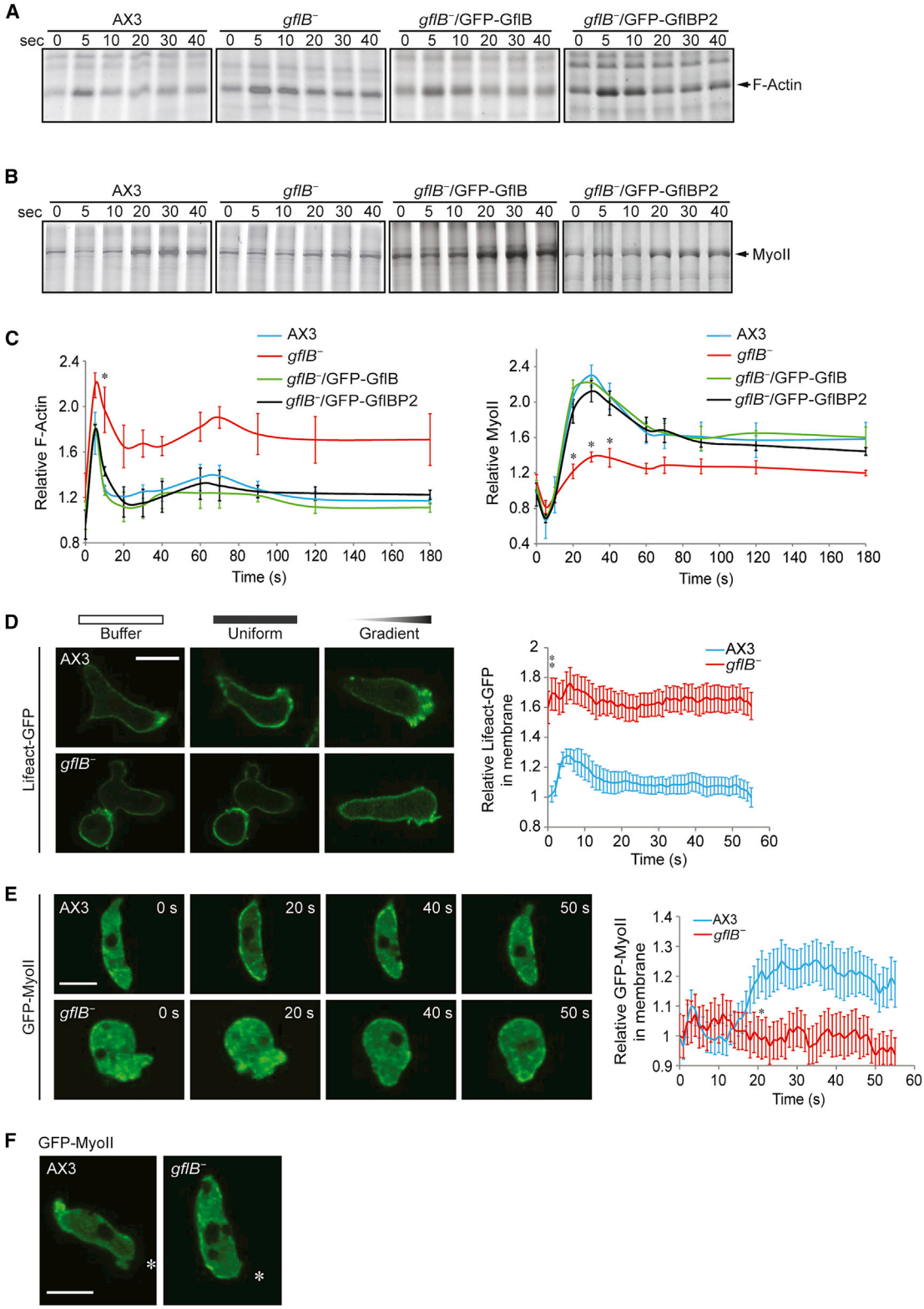

Figure 4. GflB Regulates Myosin II Assembly and Actin Polymerization

(A and B) 1 μM cAMP induced F-actin polymerization (A) and MyoII assembly (B) in AX3, *gflB*⁻, and *gflB*⁻ cells expressing GFP-GflB and GFP-GflBP2.

(C) Quantification of relative F-actin and MyoII from at least three independent experiments, representing the mean ± SD normalized to unstimulated AX3 at time 0. *p < 0.05, Student's t test.

(legend continued on next page)

cAMP chemotaxis receptor pathway (involved in aggregation and development). GflB binds to Gα2 and not Gα4, which couples to the folate GPCR used as a food-foraging receptor. The activation of GflB through a specific Gα, but not the sole Gβγ subunit, provides a mechanism for *Dictyostelium* cells to respond differently to distinct chemoattractants.

Binding of active Gα-GTP to the N terminus of GflB initiates recruitment of GflB to the leading edge and releases the auto-inhibition (Figure 6B), allowing the GEF domain to bind and stimulate the exchange activity of Rap1. In an extracellular gradient, GflB strongly localizes at the leading edge, while the activation of Gα2 is only proportional to the steepness of the gradient (Janetopoulos et al., 2001; Ueda et al., 2001). It is therefore unlikely that only binding of Gα2 to the N terminus is responsible for the accumulation of GflB to the leading edge. Furthermore, the constitutively active GflBP2 fragment and the N terminus of GflB are exclusively localized at the cortex and cell membrane, respectively. Together, these data suggest that the leading edge localization of GflB is initiated by Gα-mediated lipid binding of the N-terminal domain of GflB, followed by localization to the cell cortex via binding of GflBP2 domain. Subsequently, active GflB regulates cytoskeletal reorganization, resulting in recruitment of additional GflB to the cortex. Interestingly, F-actin also regulates PI3K localization at the leading edge via a similar positive feedback loop mechanism (Funamoto et al., 2002). So far, we have been unable to determine whether the inactive RhoGAP domain or the RasGEF domain is responsible for binding to the cell cortex. However, it is tempting to speculate that, by analogy to human OCRL (Mehta et al., 2014), binding to Rac protein via the catalytic inactive RhoGAP domain plays an important role in this process. The extent and timing of the GflB translocation to the cortex and leading edge is further fine-tuned by the phosphorylation state of the N terminus of GflB by GSK-3; non-phosphorylatable GFP-GflB protein translocation exhibits a more rapid translocation upon cAMP stimulation, consistent with constitutive inhibitory phosphorylation by GSK-3. Furthermore, our proteomic observations suggest that the Ser^{197} GSK-3 site of GflB shows increased phosphorylation at 60 s after cAMP stimulation, which might suggest that GSK-3 regulates GflB inactivation rather than activation in response to cAMP at the leading edge. The exact mechanism by which phosphorylation of the N terminus of GflB attenuates localization remains to be determined but might involve allosteric regulation of exposure of the lipid binding and/or RhoGAP domain.

Although human Rap1 was initially identified as a suppressor of Ras signaling, recent studies in various model systems have revealed several downstream pathways that are activated by both Rap1 and Ras or are activated by Rap1 independent of Ras (Frische and Zwartkruis, 2010; Kitayama et al., 1989; Kortholt et al., 2010; Mishra et al., 2005; Schwamborn and Püschel, 2004). Furthermore, studies in both mammals and *Dictyostelium* have also shown that Ras and Rap1 activation are strongly interconnected (Bolourani et al., 2008; Lee et al., 2011). Importantly, not only the individual levels of, but also the balance between, Ras and Rap1 activation are important for many processes (Ye and Carew, 2010; Ye et al., 2008) (Figure 6B). GflB is key for the balance between Ras and Rap1 activation at the leading edge of chemotaxing *Dictyostelium* cells. GflB functions as a Rap-specific GEF whose activation is mediated by direct binding of Gα2-GTP. The exact mechanism by which GflB regulates Ras activation is not completely understood but requires a functional cytoskeleton. Therefore, cells lacking *gflB* have impaired spatial and temporal Rap1 and Ras activation, which together results in uncoordinated and/or extended activation of the downstream pathways and impaired coordination of cytoskeletal rearrangements (Figure 6A). Rap1 act as a global regulator of a large number of processes crucial for *Dictyostelium*, including actin, myosin and microtubule filament formation, adhesion, and protrusion formation (Jeon et al., 2007b; Kortholt et al., 2006, 2010; Plak et al., 2013) (Figure 6B). During chemotaxis, Rap1 activation is restricted to a broad patch at the leading edge, whereby activation of the Rap-effector Phg2 it inhibits myosin filament formation. The spatial activation of Rap1 thus allows myosin filament formation only at the sites with lowest Rap1 activity (the back and sides of the cell) (Jeon et al., 2007a, 2007b). Ras, which is activated in a narrow patch at the leading edge, and Rap both stimulate actin filament formation at the front of the cell and thereby facilitate directional movement (Figure 6C).

Together, our findings indicate that GflB provides a direct link from Gα activation to localized monomeric G-protein signaling and localized cytoskeletal rearrangement, and is therefore important for *Dictyostelium* development and chemotaxis.

EXPERIMENTAL PROCEDURES

Cell Culture

All GflB mutants were derived from the axenic *Dictyostelium discoideum* AX3 strain, designated here as wild-type. *Dictyostelium* cells were maintained in HL5-C medium including glucose either on plastic Petri dishes or shaking suspension at 150 rpm at 21°C to a density of no more than 2×10^6 cells/ml. For selection, the respective antibiotics were added at a concentration of 10 μg/ml. For acquisition of developmentally competent cells capable of responding to cAMP as a chemoattractant, log-phase vegetative cells were harvested by low-speed centrifugation (300 × *g* for 3 min), washed twice, and resuspended at a density of 5×10^6 cells/ml with 12 mM Na/K phosphate buffer (PB), and pulsed with 7.5 μM cAMP solution for 5.5 hr at 6-min intervals. Subsequently, cells were collected and suspended in PB buffer. The density of cells grown in suspension was determined every 12 hr over a 7-day period, and the doubling times were obtained from growth rates that occurred during log-phase growth. For measurement of the rate of macropinocytosis, cells were shaken in 8 ml of HL5 medium at a density of 10^6 cells/ml. 20 mg of fluorescein isothiocyanate-dextran was added and 500-μl samples

(D) Translocation kinetics of the F-actin reporter Lifeact-GFP in AX3 and *gflB*$^-$ cells in response to uniform (1 μM) and gradient (10 μM) cAMP stimulation. Scale bar represents 5 μm. Quantitation of the relative fluorescence intensity of membrane-localized GFP-Lifeact is shown in the right panel, taking the starting point in AX3 cells as 1.0. Data represent mean (n = 29) ± SD of cells from three independent experiments. **$p < 0.01$, Student's t test.

(E) Live imaging of GFP-MyoII expressed in AX3 and *gflB*$^-$ cells in response to 1 μM uniform cAMP. Images captured at 1-s intervals and frames at selected time points are shown. Scale bar represents 5 μm. Quantitation of the relative fluorescence intensity of membrane-localized GFP-MyoII is shown in the right panel, taking the starting point in AX3 cells as 1.0. Data represent mean (n = 26) ± SD of cells from three independent experiments. *$p < 0.05$, Student's t test.

(F) Live imaging of translocation of GFP-MyoII expressed in AX3 and *gflB*$^-$ cells upon gradient cAMP (10 μM) stimulation. Asterisks indicate the place of the cAMP source. Scale bar represents 5 μm.

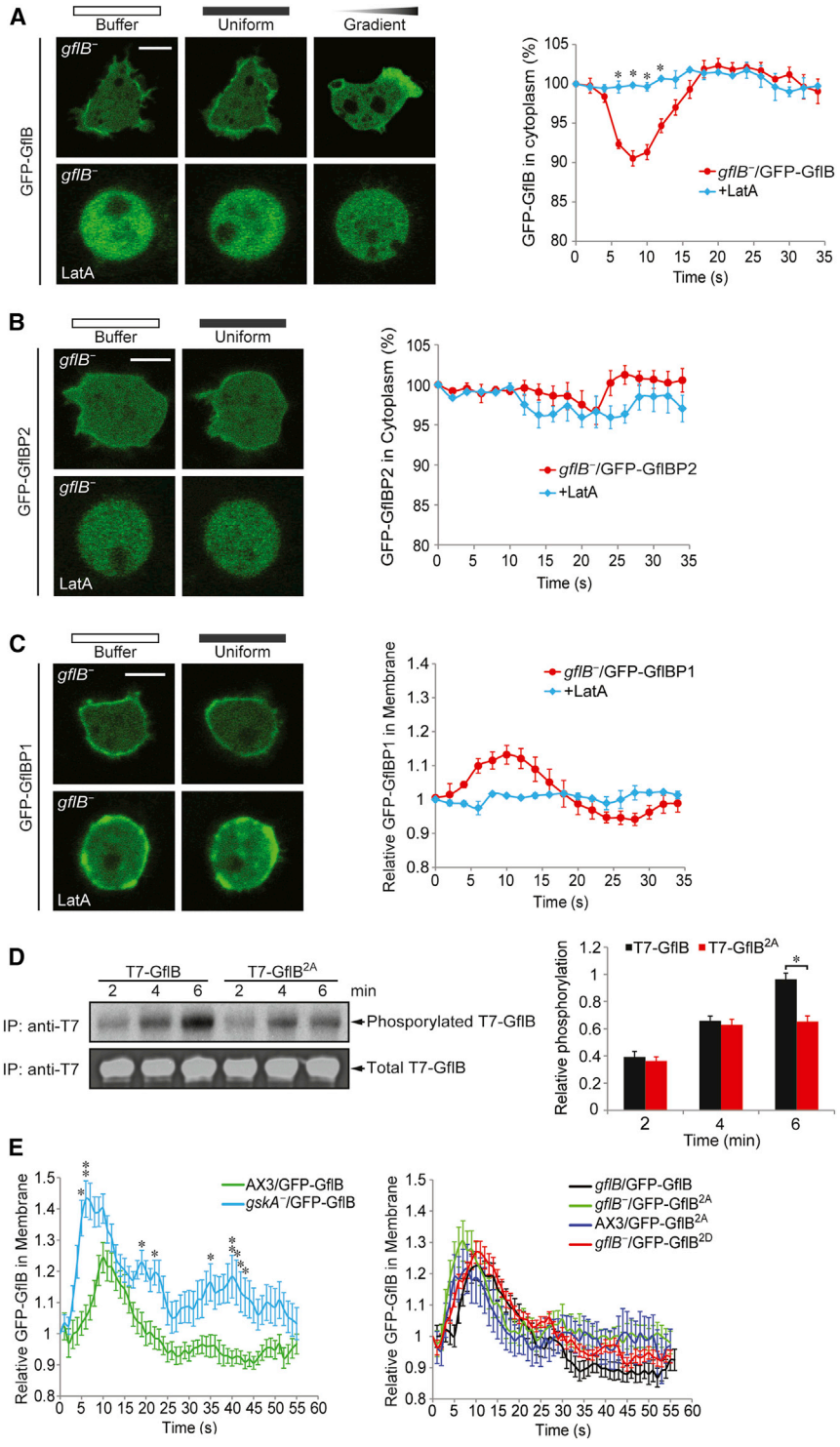

Figure 5. Regulation of GflB by N Terminus and GSK-3

(A) Live imaging of GFP-GflB expressed in *gflB*$^-$ cells with (bottom) or without (top) 5 μM LatA treatment upon uniform (1 μM) and gradient (10 μM) cAMP stimulation. The relative cytosolic fluorescence intensity of GFP-GflB is shown in the right panel. Data represent mean (n = 21) ± SEM. *p < 0.05, Student's t test. Scale bar represents 5 μm.

(B and C) Live imaging of LatA treated (bottom) and untreated (top) *gflB*$^-$ cells expressing GFP-GflBP1 and GFP-GflBP2 upon uniform 1 μM cAMP stimulation. Scale bars represent 5 μm. Translocation kinetics of GFP-GflBP1 and GFP-GflBP2 are shown in the right panels, representing mean (n = 10) ± SEM.

(D) In vitro GSK-3 kinase assay. Phosphorylation of T7-GflB and T7-GflB^{2A} (carrying two Ala mutations in the GSK-3 phosphorylation site) in the presence of [γ-^{32}P]ATP and human recombinant GSK-3β was examined for the indicated time points. Quantification is shown in the right panel, representing mean ± SD from three independent experiments. *p < 0.05, Student's t test.

(E) 1 μM cAMP-stimulated translocation kinetics of GFP-GflB expressed in AX3 and *gskA*$^-$ cells (left panel), and GFP-GflB expressed in *gflB*$^-$, GFP-GflB$^{S197A/T201A}$ expressed in AX3 and *gflB*$^-$ cells, and GFP-GflB$^{S197D/T201D}$ expressed in *gflB*$^-$ cells (right panel). Data represent mean (n = 15) ± SD of relative fluorescence intensity of membrane-localized protein taken the starting point as 1.0. *p < 0.05, **p < 0.01, Student's t test.

See also Figure S4.

et al., 2011; Plak et al., 2014; Sasaki et al., 2004). The indicated GflB overexpressing and knockout constructs were generated (Supplemental Experimental Procedures) and subsequently transformed into *Dictyostelium* cells by electroporation. Three independent, clonally isolated *gflB*$^-$ strains were used for the subsequent analysis. GflB-GEF (amino acids 644–1,282), Rap1, and RasG were expressed from a pGEX4T1 plasmid containing an N-terminal GST (GE Healthcare) in Rosetta2 (DE3) *Escherichia coli* (Novagen). Protein expression was induced with 0.1 mM isopropyl 1-thio-β-D-galactopyranoside at room temperature for 16 hr. Bacterial cell pellets were resuspended in buffer containing 50 mM Tris (pH 7.5), 50 mM NaCl, 5 mM $MgCl_2$, and 1 mM phenylmethylsulfonyl fluoride, supplemented with 1 mg/ml crushed protease inhibitor tablets (Roche), and lysed by sonication. Proteins were isolated by GSH affinity as described previously (Kortholt et al., 2006). The purified proteins were analyzed by SDS-PAGE, and the concentration was determined by Bradford's method (Bio-Rad).

were taken at t = 0, 15, 30, 45, 60, 120, and 180 min. Samples were pelleted, washed once in PB, and resuspended in lysis buffer (50 mM KCl, 10 mM Tris [pH 8.3], 2.5 mM $MgCl_2$, 0.45% Triton X-100, 0.45% Tween 20). Fluorescence was measured using a fluorimeter (470 nm excitation, 515 nm emission).

Plasmid and Protein Preparation

The GFP-PI3K, PH_{CRAC}-GFP, GFP-Lifeact, GFP-MyoII, Raf1-RBD-GFP, and RalGDS-GFP cellular markers were reported previously (Kortholt

Co-immunoprecipitation Experiments and Phospholipid Binding Assay

Co-immunoprecipitation assays are described in detail in Supplemental Experimental Procedures and were performed as described previously (Kataria et al., 2013; Kortholt et al., 2012). Lipid dot-blot assays were done using PIP

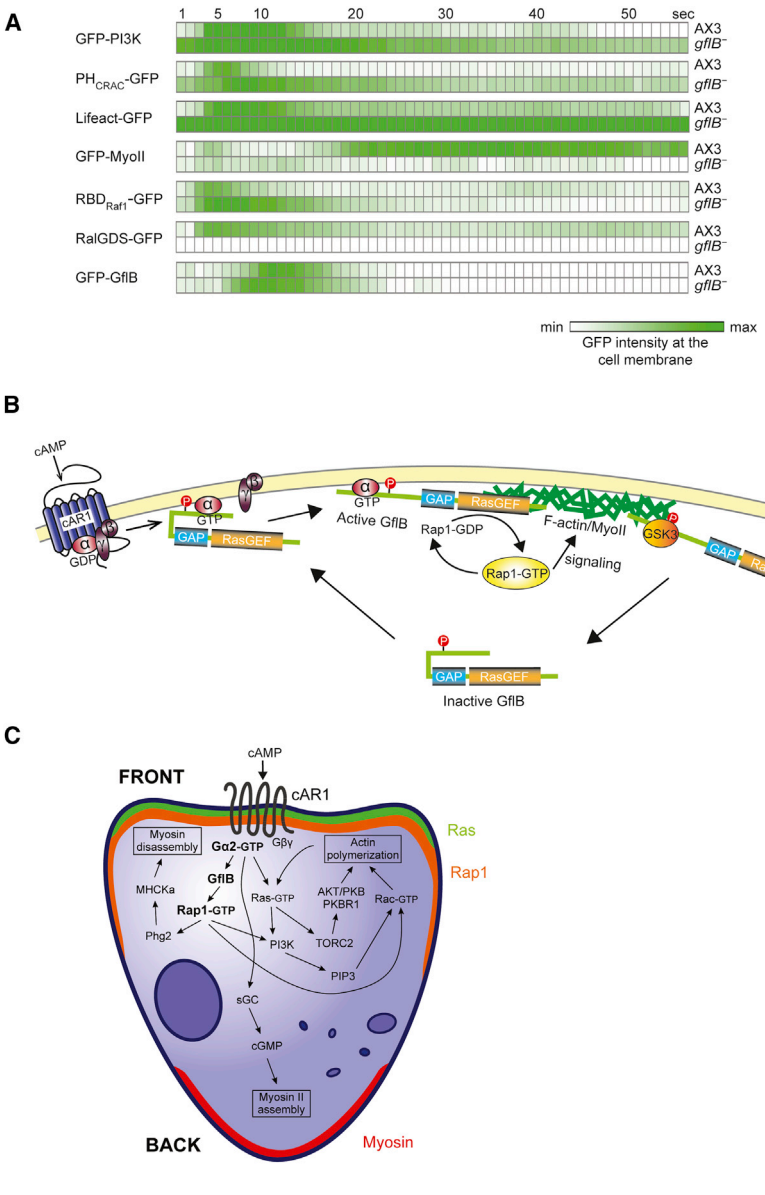

Figure 6. Model for the Activation Mechanism and Function of GflB

(A) Overview of the spatial and temporal cAMP-mediated responses of the indicated markers in AX3 and *gflB*$^{-}$ cells.

(B) Cartoon depicting the activation cycle of GflB. The N terminus keeps GflB in an inactive state in the cytoplasm. Chemoattractant stimulation induces the disassociation of the heterotrimeric G protein to the Gα-GTP and Gβγ subunits. Binding of active Gα-GTP to the N terminus of GflB releases the auto-inhibition and initiates recruitment of GflB to the leading edge, which is followed by localization to the cell cortex via binding of the GflBP2 part. Release of auto-inhibition allows the GEF domain to bind and stimulate the exchange activity of Rap1, which induces major rearrangement of the cytoskeleton and subsequently in the recruitment of additional GflB to the leading edge. GSK-3 phosphorylation at amino acids 197 and 201 (red highlighted P) regulates the extent and timing of GflB to the leading edge.

(C) Schematic of the GflB-mediated signaling pathways. Gα2-mediated GflB activation is key for the balance between Ras and Rap1 activation at the leading edge of chemotaxing *Dictyostelium* cells. Activated Rap promotes myosin disassembly at the leading edge through various downstream pathways. At the same time lower levels of active Rap1 at the side and back of the cell allow myosin assembly, thereby establishing forces for the contraction of the cell's posterior. Ras and Rap both stimulate actin filament formation at the front of the cell and thereby facilitate directional movement.

strips (Echelon Biosciences) according to the manufacturer's instructions. In brief, 1 × 10^{8} GFP-GflBP1-expressing cells were resuspended in 1 ml of lysis buffer. The PIP strips were pre-blocked with Tris-buffered saline and Tween 20 (TBST) containing 3% fatty acid free BSA (Sigma-Aldrich) for 1 hr at room temperature and subsequently incubated with 5 ml of TBST containing 50 ng of protein of the cleared GFP-GflBP1 lysate. Proteins were visualized by western blotting using an anti-GFP antibody (Santa-Cruz Biotechnology, 1:2,000 dilutions in blocking buffer) or anti-GST antibody.

In Vitro Guanine Nucleotide Exchange Assay

3 μM purified GST-Rap1 or GST-RasG was incubated overnight at 4°C in assay buffer containing 40-fold ^{3}H-labeled GDP (0.925 MBq/assay, PerkinElmer). The exchange activity was measured at room temperature with and without 6 μM GflB-GEF protein. The reaction was started by addition of 200-fold excess unlabeled GDP, and samples were taken at the indicated points. Samples were spotted on nitrocellulose filters (BA 85, Millipore), washed with 20 ml of ice-cold assay buffer, and dried before scintillation counting (PerkinElmer).

Ras and Rap1 Activation Assays

Rap1 and Ras activation was quantified in cell lysates using the previously described GST-RalGDS (Jeon et al., 2007b) and GST-RBD (Kae et al., 2007) pull-down assays, respectively. In brief, pre-cleared *Dictyostelium* cell lysates (see above) were mixed with 100 μg of recombinant purified GST-RBD or GST-RBD (RalGDS) (Kortholt et al., 2006). The samples were incubated with GSH beads for 1 hr at 4°C and subsequently washed three times with lysis buffer. Bound proteins were eluted by boiling in 1× SDS buffer and resolved on SDS-PAGE gels. Ras and Rap1 proteins were visualized by western blotting with the anti-Pan Ras (Pierce, Thermo Fisher Scientific) and anti-Rap1 antibodies. Image analysis was carried out using ImageJ software (NIH). All assays were repeated at least three times.

Development, Chemotaxis, and Live Imaging

Cells were harvested from plates at a log-phase density, washed, and suspended at a density of 3 × 10^{7} cells/ml in PB buffer to monitor the development of *Dictyostelium*. Serial dilutions of 30-μl drops were placed on PB non-nutrition agar plates and development was monitored for 24 hr at room temperature using a stereoscopic zoom microscope (SMZ-U, Nikon). Chemotaxis of *Dictyostelium* cells toward cAMP was analyzed as described previously (Sasaki et al., 2004) and quantified by DIAS (dynamic image analysis system) software (Wessels et al., 1998). Chemotaxis toward 1 μM folate with a pipette-tip opening of 3 μm and a pressure of 2 hPa (Femtojet), was measured as previously described (Kataria et al., 2013). Live confocal images were recorded using a Zeiss LSM 510 Metanlo confocal laser scanning microscope equipped with a Zeiss plan-apochromatic 63× numerical aperture 1.4 objective. The quantification of fluorescence intensity was done as described previously (Kortholt et al., 2011). Experiments were repeated independently at least three times, always assaying wild-type cells as a control for comparison in each experiment.

In Vitro PKB/PKBR1 Phosphorylation Assay

Phosphorylation immunoblot assays of PKB and PKBR1 were performed as described previously (Meili et al., 1999). In brief, samples of unstimulated and stimulated (1 μM cAMP) developed cells were taken at the indicated time points, lysed, run on SDS-PAGE gels, and transferred to nitrocellulose membranes. Phosphorylation of Akt/PKB and PKBR1 at the HM was detected using α-phospho-p70S6 kinase antibody (Cell Signaling Technology), and phosphorylation at the AL was detected using α-phosphoprotein kinase C (pan) antibody (Cell Signaling) (Kamimura et al., 2008). Western blots were quantified using ImageJ. Experiments were repeated independently at least three times, always assaying wild-type cells as a control for comparison in each experiment.

F-Actin Polymerization and MyoII Assembly

Developmentally competent cells were stimulated with 1 μM cAMP, samples were taken at the indicated time points, and cytoskeletal proteins were isolated as described previously (Steimle et al., 2001). The samples were separated on SDS-PAGE and stained with Coomassie blue. Protein amounts were quantified using ImageJ.

In Vitro GSK-3 Kinase Assay

Extracts from *gskA*$^{-}$ (GSK-3 null) cells expressing T7-GflB or T7-GflB$^{S197A/T201A}$ were mixed and immunoprecipitated with T7-tag antibody agarose beads (Novagen). The immune complexes were washed three times with cold lysis buffer and twice with cold kinase buffer (5 mM MOPS [pH 7.2], 2.5 mM β-glycerophosphate, 1 mM EGTA, 0.4 mM EDTA, 4 mM $MgCl_2$, 0.05 mM DTT, 40 ng/μl BSA) and then incubated with 30 ng of human recombinant GSK-3β (Cell Signaling). The kinase reactions were performed for up to 30 min at room temperature in the presence of radioactively labeled [γ-^{32}P] ATP (250 μM, 2 μCi/μl). The reactions were terminated by the addition of 2× SDS sample buffer. Samples were boiled and loaded on SDS-PAGE gels. The results were visualized by exposing to HyBlotCL autoradiography film (Denville Scientific).

SUPPLEMENTAL INFORMATION

Supplemental Information includes Supplemental Experimental Procedures, five figures, and three movies and can be found with this article online at http://dx.doi.org/10.1016/j.devcel.2016.05.001.

AUTHOR CONTRIBUTIONS

R.A.F. and A.K. designed the experiments and wrote the paper. Y.L. and J.L. performed most biochemical and cellular experiments, made figures, and actively contributed to writing the paper. D.M.V. and Y.L. performed microscopy experiments, P.J.M.v.H. quantified in vivo Ras activation, and F.F. performed mass spectrometry analysis. All authors read and approved the final manuscript.

ACKNOWLEDGMENTS

We wish to thank Ineke Keizer-Gunnink, Katarzyna Plak, and Kimberly Baumgardner for technical assistance. This work is supported by a CSC fellowship to Y.L., a Fulbright-MEC postdoctoral grant to J.L., an NWO-VIDI grant to A.K., and USPHS grants R01 GM037830 and P01 GM07586 to R.A.F.

Received: August 24, 2015
Revised: February 15, 2016
Accepted: April 29, 2016
Published: May 26, 2016

REFERENCES

Artemenko, Y., Lampert, T.J., and Devreotes, P.N. (2014). Moving towards a paradigm: common mechanisms of chemotactic signaling in *Dictyostelium* and mammalian leukocytes. Cell Mol. Life Sci. *71*, 3711–3747.

Arthur, W.T., Quilliam, L.A., and Coopers, J.A. (2004). Rap1 promotes cell spreading by localizing Rac guanine nucleotide exchange factors. J. Cell Biol. *167*, 111–122.

Bolourani, P., Spiegelman, G.B., and Weeks, G. (2006). Delineation of the roles played by RasG and RasC in cAMP-dependent signal transduction during the early development of *Dictyostelium discoideum*. Mol. Biol. Cell *17*, 4543–4550.

Bolourani, P., Spiegelman, G., and Weeks, G. (2008). Rap1 activation in response to cAMP occurs downstream of ras activation during *Dictyostelium* aggregation. J. Biol. Chem. *283*, 10232–10240.

Bourne, H., Sanders, D., and McCormick, F. (1991). The GTPase superfamily: conserved structure and molecular mechanism. Nature *349*, 117–127.

Cai, H., and Devreotes, P.N. (2011). Moving in the right direction: how eukaryotic cells migrate along chemical gradients. Semin. Cell Dev. Biol. *22*, 834–841.

Charest, P.G., Shen, Z., Lakoduk, A., Sasaki, A.T., Briggs, S.P., and Firtel, R.A. (2010). A Ras signaling complex controls the RasC-TORC2 pathway and directed cell migration. Dev. Cell *18*, 737–749.

Faix, J., and Weber, I. (2013). A dual role model for active Rac1 in cell migration. Small GTPases *4*, 110–115.

Frische, E.W., and Zwartkruis, F.J.T. (2010). Rap1, a mercenary among the Ras-like GTPases. Dev. Biol. *340*, 1–9.

Funamoto, S., Meili, R., Lee, S., Parry, L., and Firtel, R. (2002). Spatial and temporal regulation of 3-phosphoinositides by PI 3-kinase and PTEN mediates chemotaxis. Cell *109*, 611–623.

Hadwiger, J.A., Lee, S., and Firtel, R.A. (1994). The G alpha subunit G alpha 4 couples to pterin receptors and identifies a signaling pathway that is essential for multicellular development in *Dictyostelium*. Proc. Natl. Acad. Sci. USA *91*, 10566–10570.

Insall, R., Kuspa, A., Lilly, P.J., Shaulsky, G., Levin, L.R., Loomis, W.F., and Devreotes, P. (1994). CRAC, a cytosolic protein containing a pleckstrin homology domain, is required for receptor and G protein-mediated activation of adenylyl cyclase in Dictyostelium. J. Cell Biol. *126*, 1537–1545.

Janetopoulos, C., Jin, T., and Devreotes, P. (2001). Receptor-mediated activation of heterotrimeric G-proteins in living cells. Science *291*, 2408–2411.

Jeon, T.J., Lee, D.J., Lee, S., Weeks, G., and Firtel, R.A. (2007a). Regulation of Rap1 activity by RapGAP1 controls cell adhesion at the front of chemotaxing cells. J. Cell Biol. *179*, 833–843.

Jeon, T.J., Lee, D.J., Merlot, S., Weeks, G., and Firtel, R.A. (2007b). Rap1 controls cell adhesion and cell motility through the regulation of myosin II. J. Cell Biol. *176*, 1021–1033.

Jin, T. (2013). Gradient sensing during chemotaxis. Curr. Opin. Cell Biol. *25*, 532–537.

Kae, H., Lim, C., Spiegelman, G., and Weeks, G. (2004). Chemoattractant-induced Ras activation during *Dictyostelium* aggregation. EMBO Rep. *5*, 602–606.

Kae, H., Kortholt, A., Rehmann, H., Insall, R.H., Van Haastert, P.J.M., Spiegelman, G.B., and Weeks, G. (2007). Cyclic AMP signalling in *Dictyostelium*: G-proteins activate separate Ras pathways using specific RasGEFs. EMBO Rep. *8*, 477–482.

Kamakura, S., Nomura, M., Hayase, J., Iwakiri, Y., Nishikimi, A., Takayanagi, R., Fukui, Y., and Sumimoto, H. (2013). The cell polarity protein mInsc regulates neutrophil chemotaxis via a noncanonical G protein signaling pathway. Dev. Cell *26*, 292–302.

Kamimura, Y., Xiong, Y., Iglesias, P.A., Hoeller, O., Bolourani, P., and Devreotes, P.N. (2008). PIP3-independent activation of TorC2 and PKB at the cell's leading edge mediates chemotaxis. Curr. Biol. *18*, 1034–1043.

Kataria, R., Xu, X., Fusetti, F., Keizer-Gunnink, I., Jin, T., van Haastert, P.J.M., and Kortholt, A. (2013). *Dictyostelium* Ric8 is a nonreceptor guanine exchange factor for heterotrimeric G proteins and is important for development and chemotaxis. Proc. Natl. Acad. Sci. USA *110*, 6424–6429.

Kitayama, H., Sugimoto, Y., and Matsuzaki, T. (1989). A ras-related gene with transformation suppressor activity. Cell *56*, 77–84.

Kölsch, V., Shen, Z., Lee, S., Plak, K., Lotfi, P., Chang, J., Charest, P.G., Romero, J.L., Jeon, T.J., Kortholt, A., et al. (2013). Daydreamer, a Ras effector and GSK-3 substrate, is important for directional sensing and cell motility. Mol. Biol. Cell *24*, 100–114.

Kortholt, A., and van Haastert, P.J.M. (2008). Highlighting the role of Ras and Rap during *Dictyostelium* chemotaxis. Cell Signal. *20*, 1415–1422.

Kortholt, A., Rehmann, H., Kae, H., Bosgraaf, L., Keizer-Gunnink, I., Weeks, G., Wittinghofer, A., and Van Haastert, P.J.M. (2006). Characterization of the GbpD-activated Rap1 pathway regulating adhesion and cell polarity in *Dictyostelium discoideum*. J. Biol. Chem. *281*, 23367–23376.

Kortholt, A., Bolourani, P., Rehmann, H., Keizer-Gunnink, I., Weeks, G., Wittinghofer, A., and Van Haastert, P.J.M. (2010). A Rap/phosphatidylinositol 3-kinase pathway controls pseudopod formation [corrected]. Mol. Biol. Cell *21*, 936–945.

Kortholt, A., Kataria, R., Keizer-Gunnink, I., Van Egmond, W.N., Khanna, A., and Van Haastert, P.J.M. (2011). *Dictyostelium* chemotaxis: essential Ras activation and accessory signalling pathways for amplification. EMBO Rep. *12*, 1273–1279.

Kortholt, A., Van Egmond, W.N., Plak, K., Bosgraaf, L., Keizer-Gunnink, I., and Van Haastert, P.J.M. (2012). Multiple regulatory mechanisms for the *Dictyostelium* Roco protein GbpC. J. Biol. Chem. *287*, 2749–2758.

Kortholt, A., Keizer-Gunnink, I., Kataria, R., and Van Haastert, P.J.M. (2013). Ras activation and symmetry breaking during *Dictyostelium* chemotaxis. J. Cell Sci. *126*, 4502–4513.

Kumagai, A., Pupillo, M., Gundersen, R., Miake-Lye, R., Devreotes, P.N., Firtel, R.A., Miakelye, R., Devreotes, P.N., and Firtel, R.A. (1989). Regulation and function of G alpha protein subunits in *Dictyostelium*. Cell *57*, 265–275.

Kunisaki, Y., Nishikimi, A., Tanaka, Y., Takii, R., Noda, M., Inayoshi, A., Watanabe, K., Sanematsu, F., Sasazuki, T., Sasaki, T., et al. (2006). DOCK2 is a Rac activator that regulates motility and polarity during neutrophil chemotaxis. J. Cell Biol. *174*, 647–652.

Lee, S., Comer, F.I., Sasaki, A., McLeod, I.X., Duong, Y., Okumura, K., Yates, J.R., Parent, C.A., and Firtel, R.A. (2005). TOR complex 2 integrates cell movement during chemotaxis and signal relay in *Dictyostelium*. Mol. Biol. Cell *16*, 4572–4583.

Lee, K.J., Hoe, H.-S., and Pak, D.T. (2011). Plk2 Raps up Ras to subdue synapses. Small GTPases *2*, 162–166.

Liao, X.H., Buggey, J., and Kimmel, A.R. (2010). Chemotactic activation of Dictyostelium AGC-family kinases AKT and PKBR1 requires separate but coordinated functions of PDK1 and TORC2. J. Cell Sci. *123*, 983–992.

Li, H., Yang, L., Fu, H., Yan, J., Wang, Y., Guo, H., Hao, X., Xu, X., Jin, T., and Zhang, N. (2013). Association between Gαi2 and ELMO1/Dock180 connects chemokine signalling with Rac activation and metastasis. Nat. Commun. *4*, 1706.

Loovers, H.M., Kortholt, A., de Groote, H., Whitty, L., Nussbaum, R.L., and van Haastert, P.J.M. (2007). Regulation of phagocytosis in *Dictyostelium* by the inositol 5-phosphatase OCRL homolog Dd5P4. Traffic *8*, 618–628.

Matsubara, K., Kishida, S., Matsuura, Y., Kitayama, H., Noda, M., and Kikuchi, A. (1999). Plasma membrane recruitment of RalGDS is critical for Ras-dependent Ral activation. Oncogene *18*, 1303–1312.

Mehta, Z.B., Pietka, G., and Lowe, M. (2014). The cellular and physiological functions of the Lowe syndrome protein OCRL1. Traffic *15*, 471–487.

Meili, R., Ellsworth, C., Lee, S., Reddy, T.B.K., Ma, H., and Firtel, R.A. (1999). Chemoattractant-mediated transient activation and membrane localization of Akt/PKB is required for efficient chemotaxis to cAMP in *Dictyostelium*. EMBO J. *18*, 2092–2105.

Meili, R., Ellsworth, C., and Firtel, R.A. (2000). A novel Akt/PKB-related kinase is essential for morphogenesis in Dictyostelium. Curr. Biol. *10*, 708–717.

Mishra, S., Smolik, S.M., Forte, M.A., and Stork, P.J.S. (2005). Ras-independent activation of ERK signaling via the torso receptor tyrosine kinase is mediated by Rap1. Curr. Biol. *15*, 366–370.

Mun, H., and Jeon, T.J. (2012). Regulation of actin cytoskeleton by Rap1 binding to RacGEF1. Mol. Cells *34*, 71–76.

Nichols, J.M., Veltman, D., and Kay, R.R. (2015). Chemotaxis of a model organism: progress with *Dictyostelium*. Curr. Opin. Cell Biol. *36*, 7–12.

Plak, K., Veltman, D., Fusetti, F., Beeksma, J., Rivero, F., Van Haastert, P.J.M., and Kortholt, A. (2013). GxcC connects Rap and Rac signaling during *Dictyostelium* development. BMC Cell Biol. *14*, 6.

Plak, K., Keizer-Gunnink, I., van Haastert, P.J.M., and Kortholt, A. (2014). Rap1-dependent pathways coordinate cytokinesis in *Dictyostelium*. Mol. Biol. Cell *25*, 4195–4204.

Sarbassov, D.D., Guertin, D.A., Ali, S.M., and Sabatini, D.M. (2005). Phosphorylation and regulation of Akt/PKB by the rictor-mTOR complex. Science *307*, 1098–1101.

Sasaki, A., and Firtel, R. (2006). Regulation of chemotaxis by the orchestrated activation of Ras, PI3K, and TOR. Eur. J. Cell Biol. *85*, 873–895.

Sasaki, A.T., and Firtel, R.A. (2009). Spatiotemporal regulation of Ras-GTPases during chemotaxis. Methods Mol. Biol. *571*, 333–348.

Sasaki, A.T., Chun, C., Takeda, K., and Firtel, R.A. (2004). Localized Ras signaling at the leading edge regulates PI3K, cell polarity, and directional cell movement. J. Cell Biol. *167*, 505–518.

Schwamborn, J.C., and Püschel, A.W. (2004). The sequential activity of the GTPases Rap1B and Cdc42 determines neuronal polarity. Nat. Neurosci. *7*, 923–929.

Steimle, P.A., Yumura, S., Côté, G.P., Medley, Q.G., Polyakov, M.V., Leppert, B., and Egelhoff, T.T. (2001). Recruitment of a myosin heavy chain kinase to actin-rich protrusions in *Dictyostelium*. Curr. Biol. *11*, 708–713.

Stephens, L., Milne, L., and Hawkins, P. (2008). Moving towards a better understanding of chemotaxis. Curr. Biol. *18*, R485–R494.

Takeda, K., Sasaki, A.T., Ha, H., Seung, H.A., and Firtel, R.A. (2007). Role of PI3 kinases in chemotaxis in *Dictyostelium*. J. Biol. Chem. *282*, 11874–11884.

Tang, W., Zhang, Y., Xu, W., Harden, T.K., Sondek, J., Sun, L., Li, L., and Wu, D. (2011). A PLCβ/PI3Kγ-GSK3 signaling pathway regulates cofilin phosphatase slingshot2 and neutrophil polarization and chemotaxis. Dev. Cell *21*, 1038–1050.

Trahey, M., and McCormick, F. (1987). A cytoplasmic protein stimulates normal N-ras p21 GTPase, but does not affect oncogenic mutants. Science *238*, 542–545.

Ueda, M., Sako, Y., Tanaka, T., Devreotes, P., and Yanagida, T. (2001). Single-molecule analysis of chemotactic signaling in *Dictyostelium* cells. Science *294*, 864–867.

Vanoni, M., Bertini, R., Sacco, E., Fontanella, L., Rieppi, M., Colombo, S., Martegani, E., Carrera, V., Moroni, A., Bizzarri, C., et al. (1999). Characterization and properties of dominant-negative mutants of the ras-specific guanine nucleotide exchange factor CDC25(Mm). J. Biol. Chem. *274*, 36656–36662.

Weeks, G., Gaudet, P., and Insall, R.H. (2005). The small GTPase superfamily. In Dictyostelium Genomics, W.J. Loomis and A. Kuspa, eds. (Horizon Bioscience), pp. 173–210.

Wessels, D., Voss, E., Von Bergen, N., Burns, R., Stites, J., and Soll, D.R. (1998). A computer-assisted system for reconstructing and interpreting the dynamic three-dimensional relationships of the outer surface, nucleus and pseudopods of crawling cells. Cell Motil. Cytoskeleton *41*, 225–246.

Wu, J., Pipathsouk, A., Keizer-Gunnink, A., Fusetti, F., Alkema, W., Liu, S., Altschuler, S., Wu, L., Kortholt, A., and Weiner, O.D. (2015). Homer3 regulates the establishment of neutrophil polarity. Mol. Biol. Cell *26*, 1629–1639.

Yan, J., Mihaylov, V., Xu, X., Brzostowski, J.A., Li, H., Liu, L., Veenstra, T.D., Parent, C.A., and Jin, T. (2012). A Gβγ effector, ElmoE, transduces GPCR signaling to the actin network during chemotaxis. Dev. Cell *22*, 92–103.

Ye, X., and Carew, T.J. (2010). Small G protein signaling in neuronal plasticity and memory formation: the specific role of ras family proteins. Neuron *68*, 340–361.

Ye, X., Shobe, J.L., Sharma, S.K., Marina, A., and Carew, T.J. (2008). Small G proteins exhibit pattern sensitivity in MAPK activation during the induction of memory and synaptic facilitation in Aplysia. Proc. Natl. Acad. Sci. USA *105*, 20511–20516.

Zhang, B., Zhang, Y., Collins, C.C., Johnson, D.I., and Zheng, Y. (1999). A built-in arginine finger triggers the self-stimulatory GTPase-activating activity of Rho family GTPases. J. Biol. Chem. *274*, 2609–2612.

Zhang, S., Charest, P.G., and Firtel, R.A. (2008). Spatiotemporal regulation of Ras activity provides directional sensing. Curr. Biol. *18*, 1587–1593.

Note Added in Proof

During the final revision of our manuscript, Senoo et al. identified GflB as a RacE binding protein with a role in chemotaxis. These findings are now published:

Senoo, H., Cai, H., Wang, Y., Sesaki, H., and Lijima, M. (2016). The novel RacE binding protein GflB sharpens Ras activity at the leading edge of migrating cells. Mol. Biol. Cell., in press. Published online March 23, 2016. http://dx.doi.org/10.1091/mbc.E15-11-0796.